Soil Dynamics and Earthquake Engineering **12** (1993) 103–112

Control of structures with friction controllable sliding isolation bearings

S. Nagarajaiah

Department of Civil Engineering, University of Missouri, Columbia, Missouri, USA

M.Q. Feng

Department of Civil Engineering, University of California, Irvine, California, USA

&

M. Shinozuka*

Department of Civil Engineering, Princeton University, Princeton, New Jersey, USA

(Received 17 February 1993; accepted 1 March 1993)

A friction controllable sliding isolation system was developed and experimentally and analytically investigated by Feng *et al.* (Feng, Q., Shinozuka, M. & Fujii, S. A. friction controllable sliding isolation system. *J. Eng. Mech., ASCE,* 1993, **119**(6), in press), the control algorithm having been developed based on a key assumption that the structural motion is always in the sliding phase. However, this assumption may not be valid in cases where the sticking phase of the structural motion dominates. In this paper a new control algorithm is developed including the effects of stick–slip phases. Effect of time delay is included in the formulation. The developed algorithm is used to evaluate the accuracy and limitations of the algorithm with continuous sliding assumption. Response to various earthquake motions, simulated using the two control algorithms, is presented. Comparisons with experimental results are also presented. Effects of stick–slip phases on the response are evaluated.

INTRODUCTION

Active control[1] of linear and nonlinear structures, by means of active mass dampers, active tendon systems. active bracing systems, and variable stiffness/damping bracing, has been developed and tested in the laboratory.[2–7] Recently full scale implementation of active control in prototype structures has been accomplished.[4,8,9] Passive systems, in the form of base isolation systems, both elastomeric and sliding isolation systems, have found widespread application.[10,11] Combined active and passive control systems, referred to as hybrid control systems, in which active mass dampers or actuators in parallel with base isolation systems are employed, have been developed recently and shown to be effective.[12–17]

A more recent novel hybrid system (see Fig. 1) developed by Feng *et al.*[12,18] consists of friction controllable sliding bearings, in which fluid under pressure inside the fluid chamber of the bearing (see Fig. 2) effectively controls the bearing pressure at the sliding interface and in turn controls the level of friction at the sliding interface. Unlike hybrid systems[14,17,19,20] in which external control forces are exerted onto the structural system by means of actuators or active mass dampers, the active control in this novel system is implemented by controlling the coefficient of friction and hence the level of friction force at the sliding interface. Feng *et al.*[12,18] conducted shake table tests and demonstrated the effectiveness and advantages of using such a hybrid system in structures for limiting the transfer of seismic force to a minimum and confining the

*To whom correspondence should be addressed.

Soil Dynamics and Earthquake Engineering 0267-7261/93/$06.00

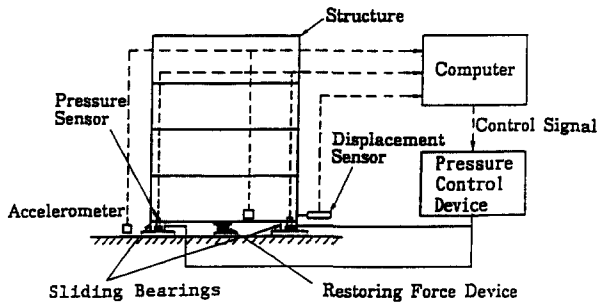

Fig. 1. Friction controllable sliding isolation system for buildings.

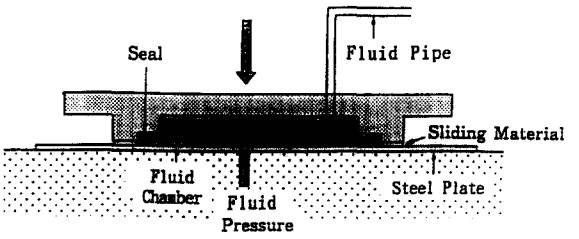

Fig. 2. Idealized view of friction controllable bearing.

sliding displacement within an acceptable range. The control algorithm used in the shake table study was developed under the key assumption that the structural motion is always in the sliding phase. This assumption was made to simplify the derivation of the control algorithm. However, this assumption may not be valid in cases where the sticking phase of the structural motion prevails over the sliding phase.[21]

In order to remove the limitation of the continuous sliding assumption, a control algorithm which can account for the stick–slip characteristics in computing the control force has to be developed. Control theories and algorithms applicable to such nonlinear and inelastic systems are limited.[12,15–17,22]

This paper presents a new control algorithm, specifically developed for the system with friction controllable bearings, based on instantaneous optimal control,[17,23] which accounts for the stick–slip phases while computing the control force. Effect of time delay is included in the formulation. The developed algorithm is used to evaluate the accuracy and limitations of the algorithm with continuous sliding assumption. Response to various earthquake motions, simulated using the two control algorithms, is presented. Comparisons with experimental results are also presented. Effects of stick–slip phases on the response are evaluated.

SYSTEM CONSIDERED

The hybrid isolation system using friction controllable sliding bearings developed by Feng *et al.*[12,18] is conceptually depicted in Fig. 1 with a building structure resting on the bearings. The idealized section view of the friction controllable sliding bearing is shown in Fig. 2. The bearing made of steel is of disk shape containing a fluid chamber, which is sealed by a rubber O-ring around the circular perimeter just inside the sliding interface. A sliding material such as PTFE plate is bonded to the steel bearing. The friction at the sliding interface between the bearing and the foundation is controlled by adjusting the pressure in the fluid inside the fluid chamber. The fluid chamber in each bearing is connected to a pressure control system composed of a servo valve, an accumulator, a hydraulic pump, a controller, and a computer. The computer calculates an appropriate signal to control the fluid pressure based on the observed structural response and sends it to the pressure control system.

ANALYTICAL MODEL

A rigid superstructure supported by the friction controllable sliding bearings is considered. Furthermore, a purely sliding system without restoring or recentering springs is considered in this study. The system can be modeled by a single-degree-of-freedom (SDOF) model. The equation of motion of this SDOF model under earthquake excitation is as follows:

$$\ddot{x} = -\ddot{x}_0 - f.\mathrm{sgn}(\dot{x}) \tag{1}$$

where

$\ddot{x}$ = relative acceleration of mass with respect to the ground,
$\ddot{x}_0$ = input earthquake acceleration,
sgn = signum function,
f = normalized friction force defined as $f = \mu g$,
μ = coefficient of friction at the sliding interface,
g = acceleration due to gravity.

The normalized friction force, f, on the sliding interface between the structure and the foundation is controlled by changing the fluid pressure in the bearing chamber by means of the pressure control system. The dynamic characteristics of the pressure control system are assumed to follow the first-order time delay model:

$$T\dot{p} + p = u \tag{2}$$

where

p = pressure in the fluid chamber of the bearing,
u = pressure control signal from the computer,
T = time constant.

The normalized friction force, f, is proportional to the pressure p in the bearing chamber:

$$f = -c_1 p + c_2 \tag{3}$$

where c_1 and c_2 are constants.

CONTROL ALGORITHMS

Two control algorithms, based on instantaneous optimal control,[17,23] are presented. First the control algorithm with continuous sliding (CS) assumption, referred to as algorithm CS, developed by Feng *et al.*[12,18] is presented briefly. Next the control algorithm with stick–slip (SS) phases included, referred to as algorithm SS, developed in this paper is presented.

Control algorithm — Continuous Sliding (CS)

The optimal pressure control signal $u(t)$ is determined by minimizing the following time dependent objective function $J(t)$ at every time instant, t, for the entire duration of an earthquake:

$$J(t) = q_d x^2(t) + q_f f^2(t) + r u^2(t) \tag{4}$$

in which the normalized friction force, f, equivalently represents the amount of response acceleration and also serves as a measure of the transfer of seismic force to the structure. The weighting coefficients q_d and q_f are non-negative and r is positive. They indicate the relative importance in the control objectives of the sliding displacement, response acceleration and pressure control signal, respectively. The basic objective of the control is to make the structure slide as much as possible within an acceptable range and at the same time to restrict the transfer of seismic force to a minimum.

The algorithm CS[12,18] is derived under the assumption that the structural motion is always in the sliding phase. The equation of motion, given by eqn (1), is used as a constraint when minimizing the objective function $J(t)$. The first-order time delay relationship between the control signal and the pressure, given in eqn (2), and the relationship between the normalized friction force and the pressure, given in eqn (3), are also used as constraints. In the formulation, however, these equations will be solved numerically using Newmark's β method, with $\beta = 1/6$, as shown below and these numerical solutions will be used as constraint:

$$x(t) = x(t-\Delta t) + \dot{x}(t-\Delta t)\Delta t + \ddot{x}(t-\Delta t)\frac{\Delta t^2}{2} + (\ddot{x}(t) - \ddot{x}(t-\Delta t))\frac{\Delta t^2}{6} \tag{5}$$

$$f(t) = f(t-\Delta t) + \dot{f}(t-\Delta t)\Delta t + (\dot{f}(t) - \dot{f}(t-\Delta t))\frac{\Delta t}{2} \tag{6}$$

Substituting eqns (5) and (6) in eqns (1)–(3):

$$x(t) = af(t)\,.\,\mathrm{sgn}(\dot{x}(t)) + b\ddot{x}_0(t) + d_1(t-\Delta t) \tag{7}$$

$$f(t) = -cu(t) + d_2(t-\Delta t) \tag{8}$$

where:

$$a = b = \frac{\Delta t^2}{6}$$

$$c = \frac{c_1 \Delta t}{2T + \Delta t}$$

$$d_1(t-\Delta t) = x(t-\Delta t) + \dot{x}(t-\Delta t)\Delta t + \tfrac{1}{3}\ddot{x}(t-\Delta t)\Delta t^2$$

$$d_2(t-\Delta t) = \frac{2T}{2T+\Delta t}\left(\frac{c_2 \Delta t}{2T} + f(t-\Delta t) + \tfrac{1}{2}\dot{f}(t-\Delta t)\Delta t\right)$$

To minimize the objective function $J(t)$, given by eqn (4), subject to the constraints given in eqns (7) and (8), the following Hamiltonian H is established, by introducing the Lagrangian multipliers λ_1 and λ_2:

$$H = q_d x^2(t) + q_f f^2(t) + r u^2(t) + \lambda_1(x(t) - af(t)\,.\,\mathrm{sgn}(\dot{x}(t)) - b\ddot{x}_0(t) - d_1(t-\Delta t)) + \lambda_2(f(t) + cu(t) - d_2(t-\Delta t)) \tag{9}$$

The necessary conditions for minimizing the objective function $J(t)$, subject to the constraint equations, are

$$\frac{\partial H}{\partial x} = 0; \quad \frac{\partial H}{\partial f} = 0; \quad \frac{\partial H}{\partial u} = 0; \quad \frac{\partial H}{\partial \lambda_1} = 0; \quad \frac{\partial H}{\partial \lambda_2} = 0 \tag{10}$$

Substituting eqns (10) into eqn (9) yields the optimal pressure control signal:

$$u(t) = F_f f(t) + F_d x(t)\,.\,\mathrm{sgn}(\dot{x}(t)) \tag{11}$$

where the control feedback gains F_f and F_d are given by

$$F_f = c\frac{q_f}{r}; \qquad F_d = ca\frac{q_d}{r} \tag{12}$$

and the displacement, $x(t)$, and normalized friction force, $f(t)$, are used for feedback purpose. Note that sgn $(\dot{x})$ can be obtained from the displacement signal without the need to measure the velocity. The friction force is difficult to measure by a sensor, but the signal from the acceleration sensor $|\ddot{x}(t) + \ddot{x}_0(t)|$ can be used instead of $f(t)$ for a rigid structure. Therefore, the control signal is given by

$$u(t) = F_f(|\ddot{x}(t) + \ddot{x}_0(t)|) + F_d x(t)\,.\,\mathrm{sgn}(\dot{x}(t)) \tag{13}$$

Equation (7), along with the stick–slip conditions and eqns (8) and (13), are used to model the system.

Control algorithm — Stick–Slip (SS)

In the development of the algorithm SS the stick–slip phases are given due consideration by using a hysteretic model for sliding interfaces.[10] The model is based on the

following differential equation proposed by Wen:[24]

$$\dot{y} = (\dot{x} - \gamma|\dot{x}|y^2 \cdot \mathrm{sgn}(\dot{x}y) - \beta\dot{x}y^2)/Y \tag{14}$$

where sgn = signum function; y = hysteretic dimensionless parameter; γ and β are dimensionless parameters; and Y = shear displacement of friction interface material before sliding commences.

The friction force normalized with respect to the mass of the structure is represented as follows:

$$f_f = \mu g y = fy \tag{15}$$

where μ = coefficient of friction; g = acceleration due to gravity; and y = hysteretic dimensionless parameter, bounded by ± 1, which accounts for the stick–slip conditions instead of the signum function.

Equation (1) can be reduced to two first-order differential equations as follows:

$$\dot{x}_1 = x_2 \tag{16}$$

$$\dot{x}_2 = -\ddot{x}_0 - fy \tag{17}$$

Equation (14) can be expressed in terms of the state variables x_2 and y as follows:

$$\dot{y} = (x_2 - \gamma|x_2|y^2 \cdot \mathrm{sgn}(x_2 y) - \beta x_2 y^2)/Y \tag{18}$$

The state variables in eqns (16)–(18) can be combined in the state vector:

$$\mathbf{z}(t) = \begin{Bmatrix} x_1 \\ x_2 \\ y \end{Bmatrix} \tag{19}$$

Equations (16)–(18) can be represented by the following nonlinear matrix equation:

$$\dot{\mathbf{z}}(t) = \mathbf{g}[\mathbf{z}(t), f(t)] + \mathbf{w}\ddot{x}_0 \tag{20}$$

where

$$\mathbf{g}[\mathbf{z}(t)] = \begin{Bmatrix} x_2(t) \\ -f(t)y(t) \\ (x_2(t) - \gamma|x_2(t)|y^2(t) \cdot \mathrm{sgn}(x_2(t)y(t)) - \beta x_2(t)y^2(t))/Y \end{Bmatrix}_{(3x1)}$$

$$\mathbf{w} = \begin{Bmatrix} 0 \\ -1 \\ 0 \end{Bmatrix}_{(3x1)}$$

The first-order nonlinear matrix equation (20) can be solved using the fourth-order Runge–Kutta method as follows:

$$\mathbf{z}(t) = \mathbf{z}(t - \Delta\tau) + (\Delta\tau/6)[\mathbf{k}_1 + 2\mathbf{k}_2 + 2\mathbf{k}_3 + \mathbf{k}_4] \tag{21}$$

in which $\Delta\tau = 2\Delta t$; Δt = time step of integration; and $\mathbf{k}_1$, $\mathbf{k}_2$, $\mathbf{k}_3$, $\mathbf{k}_4$ are vectors defined as follows:

$$\mathbf{k}_1 = \{\mathbf{g}[\mathbf{z}(t - 2\Delta t), f(t - 2\Delta t)] + \mathbf{w}\ddot{x}_0(t - 2\Delta t)\}_{(3x1)}$$

$$\mathbf{k}_2 = \{\mathbf{g}[\mathbf{z}(t - 2\Delta t) + \mathbf{k}_1\Delta t, f(t - \Delta t)] + \mathbf{w}\ddot{x}_0(t - \Delta t)\}_{(3x1)}$$

$$\mathbf{k}_3 = \{\mathbf{g}[\mathbf{z}(t - 2\Delta t) + \mathbf{k}_2\Delta t, f(t - \Delta t)] + \mathbf{w}\ddot{x}_0(t - \Delta t)\}_{(3x1)}$$

$$\mathbf{k}_4 = \{\mathbf{g}[\mathbf{z}(t - 2\Delta t) + 2\mathbf{k}_3\Delta t, f(t)] + \mathbf{w}\ddot{x}_0(t)\}_{(3x1)}$$

Equation (21) can be rewritten in the following form:

$$\mathbf{z}(t) = \mathbf{d}(t - 2\Delta t, t - \Delta t) + (\Delta t/3)[\mathbf{b}f(t) + \mathbf{w}\ddot{x}_0(t)] \tag{22}$$

where

$$\mathbf{b} = \begin{Bmatrix} 0 \\ -y(t - 2\Delta t) - 2\Delta t k_3^{(3,1)} \\ 0 \end{Bmatrix}_{(3x1)}$$

in which $k_3^{(3,1)}$ = element (3,1) of vector $\mathbf{k}_3$; and $\mathbf{d}(t - 2\Delta t, t - \Delta t)$ includes all the terms in eqn (21) excluding the second term, in square brackets, on the right-hand side of eqn (22).

In eqn (20) the vectors $\mathbf{g}[\mathbf{z}(t), f(t)]$ are functions of the state vector $\mathbf{z}(t)$ and the normalized friction force $f(t)$. Hence the vector $\mathbf{g}[\mathbf{z}(t), f(t)]$ is evaluated by substituting the elements x_1, x_2, y of the vector $\mathbf{z}(t)$ and $f(t)$. In order to evaluate the vectors $\mathbf{g}[\mathbf{z}(t - 2\Delta t) + \mathbf{k}_1\Delta t, f(t - \Delta t)]$, etc., the elements of the vector $\mathbf{z}(t - 2\Delta t) + \mathbf{k}_1\Delta t$ are used in place of the elements of the vector $\mathbf{z}(t)$, and $f(t - \Delta t)$ in place of $f(t)$.

In deriving the control algorithm the following equations are used as constraints when minimizing the objective function: (i) the numerical solution of the equation of motion, i.e. eqn (22); and (ii) the numerical solution of the first-order time delay relationship between the control signal and the normalized friction force, obtained by substituting eqn (3) into eqn (2). The equation obtained by substituting eqn (3) into eqn (2) is as follows:

$$\dot{f}(t) = (1/T)(c_2 - c_1 u(t) - f(t)) \tag{23}$$

This can be solved numerically using the fourth-order Runge–Kutta method as follows:

$$f(t) = f(t - \Delta\tau) + (\Delta\tau/6)[N_1 + 2N_2 + 2N_3 + N_4] \tag{24}$$

in which $\Delta\tau = 2\Delta t$; Δt = time step of integration; and N_1, N_2, N_3, N_4 are defined as follows:

$$N_1 = (1/T)\{c_2 - c_1 u(t - 2\Delta t) - f(t - 2\Delta t)\}$$

$$N_2 = (1/T)\{c_2 - c_1 u(t - \Delta t) - (f(t - 2\Delta t) + N_1\Delta t)\}$$

$$N_3 = (1/T)\{c_2 - c_1 u(t - \Delta t) - (f(t - 2\Delta t) + N_2\Delta t)\}$$

$$N_4 = (1/T)\}c_2 - c_1 u(t) - (f(t - 2\Delta t) + N_3 2\Delta t)\}$$

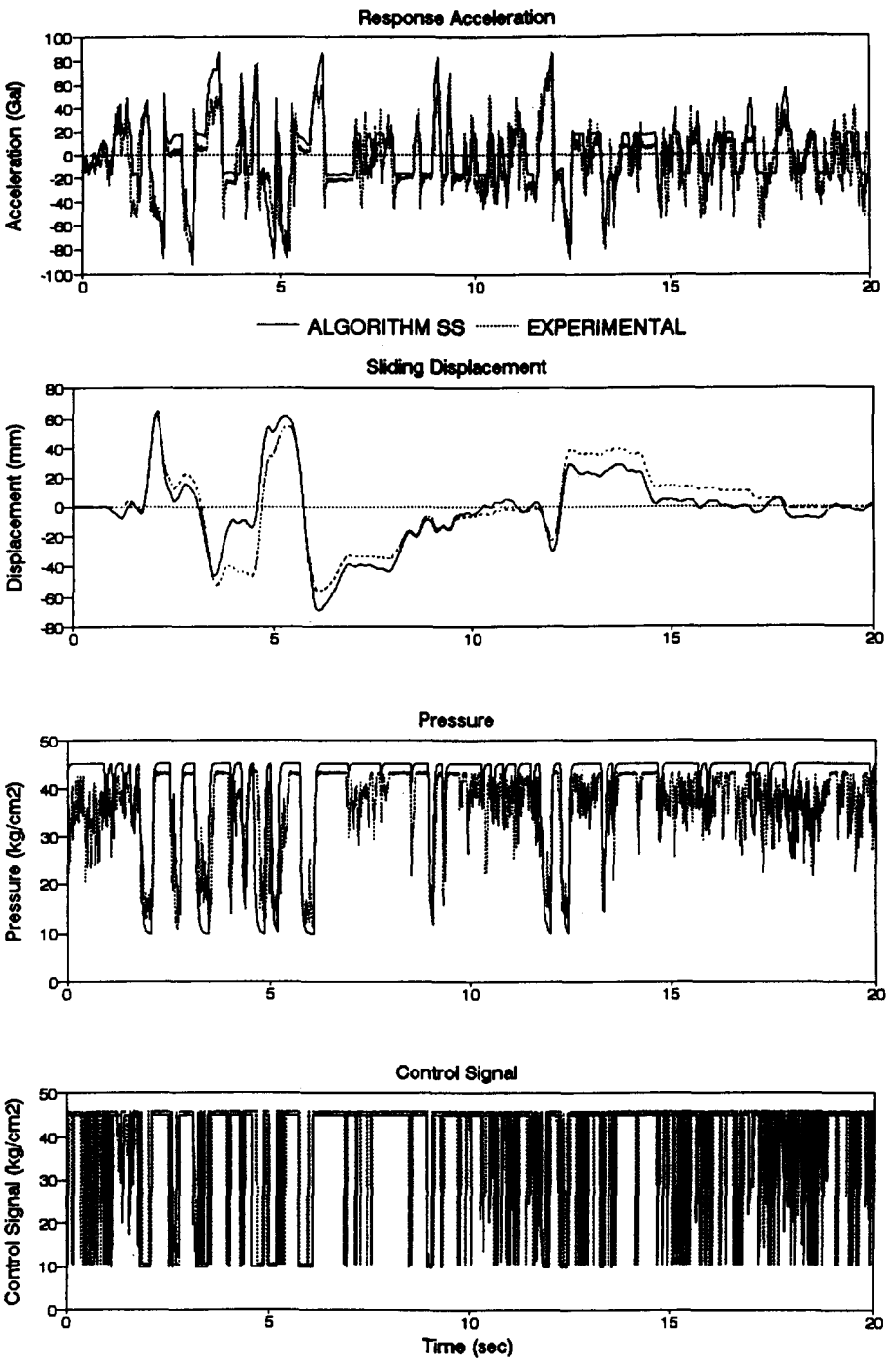

Fig. 3. Comparison of measured and simulated responses, using algorithm SS, under 1940 NS El Centro earthquake input (300 Gal). The responses shown are: response acceleration of the rigid structure; sliding displacement of the rigid structure; pressure in the bearing fluid chamber; and pressure control signal from the computer. 1 Gal = 1 cm/s^2.

Equation (24) can be rewritten in the following form:

$$f(t) = d_f(t - 2\Delta t, t - \Delta t) - c_1 u(t)\frac{\Delta t}{3T} \tag{25}$$

where $d_f(t - 2\Delta t, t - \Delta t)$ includes all the terms in eqn (24) excluding the second term on the right-hand side of eqn (25).

The optimal pressure control signal $u(t)$ is determined by minimizing the following time dependent objective function $J(t)$ at every time instant, t, for the entire duration of an earthquake:

$$J(t) = \mathbf{z}^T(t)\mathbf{Q}_d\mathbf{z}(t) + Q_f f^2(t) + Ru^2(t) \tag{26}$$

in which $\mathbf{Q}_d$ is a 3×3 positive semi-definite weighting matrix, the weighting coefficient Q_f is non-negative, and R is positive.

To minimize the objective function $J(t)$ given by eqn

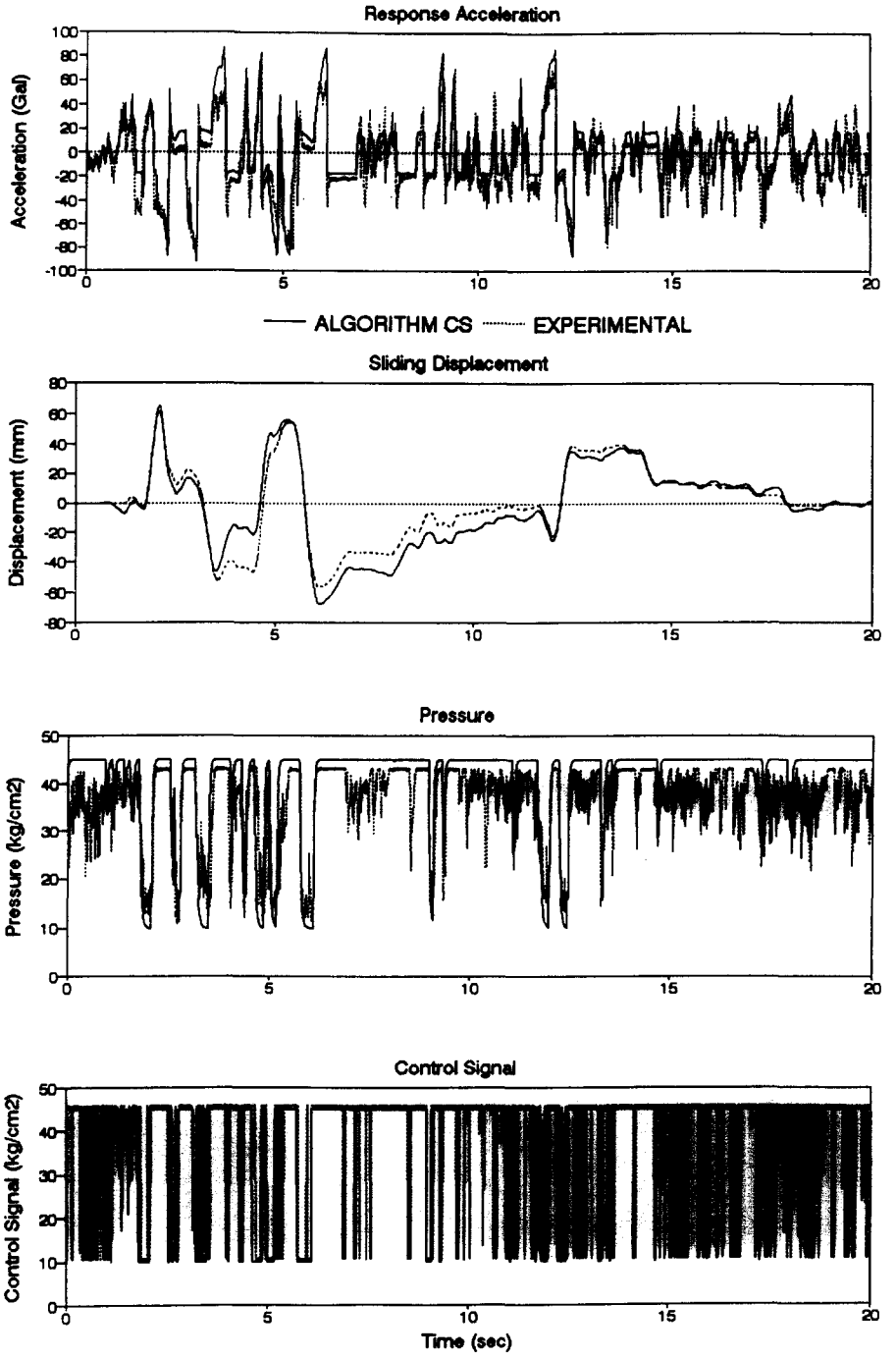

Fig. 4. Comparison of measured and simulated responses, using algorithm CS, under 1940 NS El Centro earthquake input (300 Gal).

(26), subject to constraints given by eqns (22) and (25), the following Hamiltonian H is established, by introducing the Lagrangian multiplier, vector λ_1, and λ_2:

$$H = \mathbf{z}^{\mathrm{T}}(t)\mathbf{Q}_{\mathrm{d}}\mathbf{z}(t) + Q_{\mathrm{f}}f^2(t) + Ru^2(t) + \lambda_1^{\mathrm{T}}\{\mathbf{z}(t) - \mathbf{d}(t - 2\Delta t, t - \Delta t) - (\Delta t/3)[\mathbf{b}f(t) + \mathbf{w}\ddot{x}_0(t)]\} + \lambda_2\left\{f(t) - d_{\mathrm{f}}(t - 2\Delta t, t - \Delta t) + c_1 u(t)\frac{\Delta t}{3T}\right\} \quad (27)$$

The necessary conditions for minimizing the objective function, $J(t)$, subject to the constraint equations, are the following:

$$\frac{\partial H}{\partial \mathbf{z}} = 0; \quad \frac{\partial H}{\partial f} = 0; \quad \frac{\partial H}{\partial u} = 0; \quad \frac{\partial H}{\partial \lambda_1} = 0; \quad \frac{\partial H}{\partial \lambda_2} = 0 \quad (28)$$

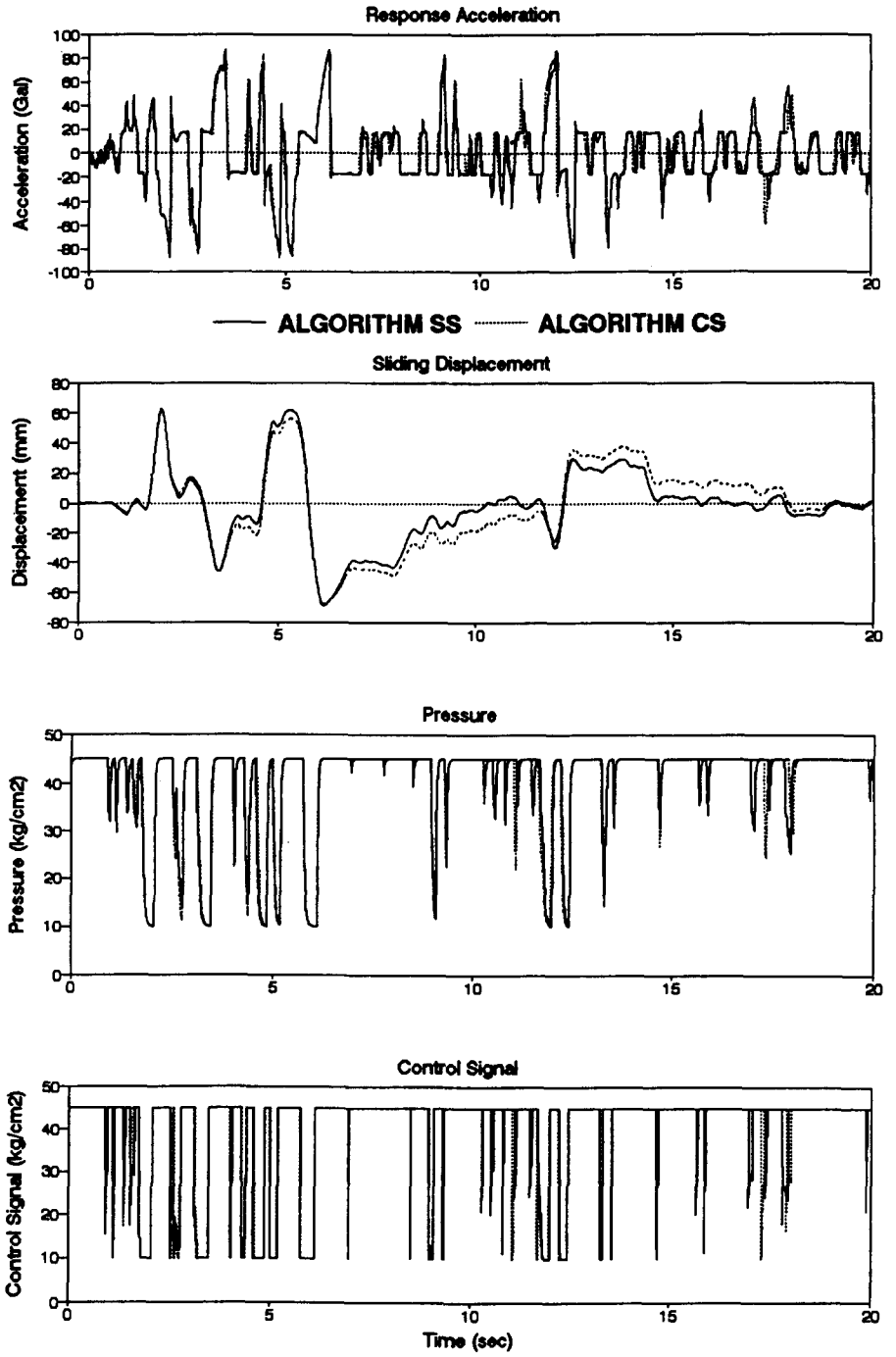

Fig. 5. Comparison of simulated responses, using algorithm SS and algorithm CS, under 1940 NS El Centro earthquake input (300 Gal).

Substituting eqns (28) into eqn (27) yields the optimal pressure control signal:

$$u(t) = c_1 \frac{\Delta t}{3TR} Q_f f(t) + c_1 \frac{\Delta t^2}{9TR} \mathbf{b}^T \mathbf{Q}_d \mathbf{z}(t) \tag{29}$$

The weighting coefficient $R = 1$. The weighting coefficient Q_f and weighting matrix $\mathbf{Q}_d$ are chosen such that gain constants identical to constants F_f and F_d in eqn (13) result, with displacement $x_1(t)$ and the normalized friction force $f(t)$ as feedback. The values of $F_f = 0{\cdot}098\,\text{N/mm}^2$ ($1\,\text{kgf/cm}^2$) and $F_d = -4{\cdot}413\,\text{N/mm}^2$ ($-45\,\text{kgf/cm}^2$) were used by Feng *et al.*[12,18] in their experiments. Since the structure considered is a purely sliding rigid structure without recentering springs, the absolute value of the acceleration $|\ddot{x}(t) + \ddot{x}_0(t)|$ is used instead of the normalized friction force $f(t)$, similar to eqn (13).

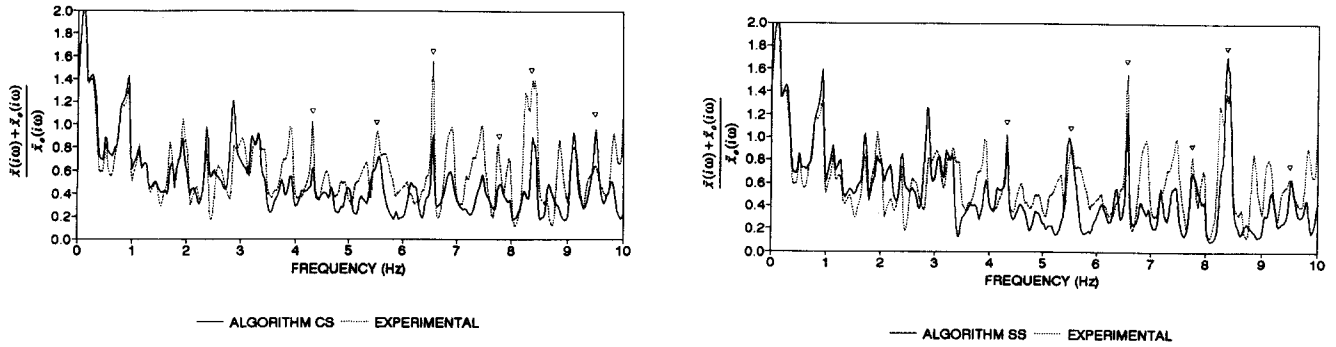

Fig. 6. Frequency response function of acceleration under 1940 NS El Centro earthquake input (300 Gal).

EVALUATION OF CONTROL ALGORITHMS CS AND SS

The control algorithm SS is implemented on the model structure tested on a shaking table by Feng *et al.*[12,18] The model, representing a rigid structure, consisted of a steel frame and steel weights. The total weight of the model was 120 kN (12 tonf). The model was supported equally by four friction controllable sliding bearings. The sliding interface of the bearing was brass sheet sliding material on stainless steel plate (see Fig. 2). The rubber O-ring used to seal the fluid chamber was 5·7 mm in diameter. The area of the sliding interface was 8600 mm^2, and the vertically projected area of the fluid chamber was 5770 mm^2. No restoring or recentering spring was used in order to study the effect of friction force only.

The pressure control signal was confined between $u_{max} = 4{\cdot}413\,N/mm^2$ (45 kgf/cm^2) and $u_{min} = 0{\cdot}9807\,N/mm^2$ (10 kgf/cm^2). The time constant T in eqn (2), identified in the experiments by Feng *et al.*,[12,18] was $T_i = 0{\cdot}029$ s under increasing pressure, or $T_d = 0.035$ s under decreasing pressure. The coefficient of friction, μ, and hence the normalized friction force, f, varied linearly with pressure and are given by eqn (3). The coefficients in eqn (3), found experimentally, i.e. $c_1 = 101{\cdot}97\,mm^3/s^2\,N$ ($2{\cdot}4\,cm^3/s^2\,kgf$) and $c_2 = 1240\,mm/s^2$, result in a coefficient of friction $\mu = 10{\cdot}2\%$ at a pressure of $0{\cdot}9807\,N/mm^2$ (10 kgf/cm^2), and $\mu = 1{\cdot}6\%$ at a pressure of $4{\cdot}413\,N/mm^2$ (45 kgf/cm^2). Furthermore, it was found by Feng *et al.*[12,18] that eqn (3) is valid at a sliding velocity of zero and that the normalized friction force depends on the sliding velocity, also, in addition to the pressure. The variation of friction with sliding velocity was found to follow the relationship

$$f = f_0 \cdot k^2/(\dot{x}^2 + k^2) \tag{30}$$

where f_0 is the normalized friction force at zero sliding velocity and is given by eqn (3), and $k = 1.1$ mm/s. It is to be noted that Feng *et al.* [12,18] found in their experiments that despite the development of control algorithms on reduced-order models, ignoring the influence of sliding velocity on the friction force, the control performance was satisfactory.

Response to El Centro excitation

The measured results from the shake table experiment

Table 1. Comparison of simulations with experimental results

Earthquake	Table accel. $\ddot{x}_0$ (Gal) (cm/s^2)	Deck response accel. $\ddot{x}$ (Gal) (cm/s^2)	Deck relative displ. x (mm)	Pressure in fluid chamber p (N/mm^2)	Peak control signal u (N/mm^2)
Experimental results					
El Centro	308·1	92·2	64·65	4·301	4·520
Hachinohe	293	104·4	76·25	4·349	4·505
Taft	268	95·81	66·92	4·332	4·505
Control algorithm CS					
El Centro	308·1	87·43	66·62	4·413	4.413
Hachinohe	293	102·1	74·02	4·413	4·413
Taft	268	93·2	68·52	4·413	4·413
Control algorithm SS					
El Centro	308·1	88·3	65·2	4·413	4·413
Hachinohe	293	103·5	75·56	4·413	4·413
Taft	268	95·32	66·26	4·413	4·413

by Feng *et al.*[12,18] for 1940 NS El Centro earthquake input, with peak table acceleration of 300 Gal (1 Gal = 10 mm/s^2), are presented in Fig. 3. This figure shows the response acceleration of the rigid structure, the sliding displacement of the rigid structure with respect to the shake table, the pressure in the bearing chamber, and the control signal. Figure 3 also shows the simulated response using algorithm SS with a time step $\Delta t = 0{\cdot}01 \times 10^{-4}$ s, $Y = 0{\cdot}0254$ mm, $\gamma = 0{\cdot}9$, and $\beta = 0{\cdot}1$. Figure 4 shows the simulated response using algorithm CS with a time step $\Delta t = 0{\cdot}002$ s. A comparison between the simulated results, using both control algorithms, and the measured results indicates good agreement, which demonstrates the accuracy of the analytical model and the control algorithms. The peak structural response acceleration, shown in Fig. 3, is significantly less than the input acceleration of 300 Gal. The peak structural response acceleration is bounded by the level of friction at the sliding interface, regardless of the input acceleration.

Figure 5 shows a comparison between the simulated results using the two algorithms, CS and SS. In Fig. 5 a negligible difference appears to be present between the response simulated using the two control algorithms. Hence to evaluate the effect of stick–slip phases on the structural response, the frequency response function for acceleration (i.e., the ratio of the rigid superstructure acceleration to the shake table acceleration) is examined in Fig. 6. The frequency response functions in the case of algorithms CS and SS are compared to that of the experiment. Note the significant reduction in acceleration and hence the seismic force transferred, over the whole frequency range. Close examination of the frequency response functions in Fig. 6 indicates that the algorithm SS captures the response in the high frequency region (indicated by arrows in Fig. 6 between 4 and 10 Hz), resulting from stick–slip phases, more accurately than does the algorithm CS. This is to be expected, since the algorithm CS assumes continuous sliding.

It can be concluded from the aforementioned observations, and from the test results of Feng *et al.*[12,18] that both algorithms will yield comparable results for rigid structures; however, algorithm SS is more accurate in the case of flexible structures.

Response to various earthquakes

Further comparisons of results of the two algorithms and the experimental results, for Hachinohe NS and Taft N21E earthquakes, are shown in Table 1. As evident from Table 1 both algorithms yield comparable results because the structure considered is rigid.

COMPARISON WITH PASSIVE SYSTEM RESULTS

Comparisons of results from the hybrid system and from the passive sliding system without control have been presented by Feng *et al.*[12,18] It was found that the hybrid system was effective in reducing the acceleration further than the passive system and was also effective in restricting the sliding displacement within acceptable limits.

CONCLUSIONS

In this paper a new control algorithm (referred to as algorithm SS) has been developed specifically for friction controllable sliding isolation system accounting for the stick–slip phases. Feng *et al.* [12,18] developed and experimentally and analytically investigated a friction controllable sliding isolation system: they developed the control algorithm (referred to as algorithm CS) with the assumption that the structural motion is always in the sliding phase.

The developed control algorithm SS has been used to evaluate the limitations of the continuous sliding assumption and to evaluate the effects of stick–slip phases. The main conclusions of the evaluation are as follows:

(1) Comparisons between the simulated results, using the two algorithms CS and SS, and the experimental results indicates good agreement, implying that the analytical model and control algorithms represent the actual system satisfactorily.
(2) It is found that the control algorithm SS captures the response in the high frequency range, resulting from stick phases, more accurately than the control algorithm CS, which is to be expected because of the continuous sliding assumption in the algorithm CS. The control algorithms yield comparable results for rigid structures; however, algorithm SS is more accurate in the case of flexible structures.
(3) Significant reduction in seismic force transfer occurs because of the friction controllable sliding isolation system: the peak structural acceleration is reduced significantly; significant acceleration reduction occurs over the whole frequency range; and the sliding displacement is restricted within acceptable limits. The peak structural response acceleration is bounded by the level of friction at the sliding interface, regardless of the input acceleration.

ACKNOWLEDGEMENTS

The first author would like to thank Professor Andrei Reinhorn for discussions during the course of this study. Partial funding for this study, from the National Center for Earthquake Engineering Research grant no. 91-2204, is gratefully acknowledged.

REFERENCES

1. Soong, T.T., T.T. *Active Structural Control: Theory and Practice*, 1st edn. Longman Scientific & Technical, Essex, UK, 1990.
2. Chong, K.P., Liu, S.C. & Li, J.C. (eds). *Intelligent Structures*, Elsevier Applied Science, New York, 1990.
3. Housner, G.W. & Masri, S.F. (eds). *Proc. US National Workshop on Structural Control Research*, University of Southern California, 1991.
4. Kobori, T. State-of-the-art of seismic response control research in Japan, *Proc. US National Workshop on Structural Control Research*, University of Southern California, 1991, pp. 1–21.
5. Reinhorn, A.M. & Manolis, G.D. Current state of knowledge on structure control, *Shock Vib. Dig.*, 1985, **17**(10), 35–41.
6. Soong, T.T., Masri, S.F. & Housner, G.W. An overview of active structural control under seismic loads, *Earthquake Spectra*, 1991, **7**, 483–505.
7. Yang, J.N. & Soong, T.T. Recent advancement in active control of civil engineering structures, *J. Probab. Eng. Mech.*, 1988, **3**(4), 179–88.
8. Reinhorn, A.M., Soong, T.T., Riley, M.A., Lin, R.C., Aizawa, S. & Higashino, M. Full scale implementation of active control part II: installation and performance, *J. Struct. Eng., ASCE*, 1992, **119**(2), 1935–60.
9. Soong, T.T., Reinhorn, A.M., Wang, Y.P. & Lin, R.C. Full scale implementation of active control part I: design, *J. Struct. Eng., ASCE*, 1991, **117**(11), 3516–35.
10. Constantinou, M.C., Mokha, A.S. & Reinhorn, A.M. Teflon bearings in base isolation. II: Modeling, *J. Struct. Eng., ASCE*, 1990, **116**(2), 455–74.
11. Kelly, J.M. Aseismic base isolation; review and bibliography, *J. Soil Dyn. Earth. Eng.*, 1986, **5**(3), 202–16.
12. Feng, Q., Shinozuka, M. & Fujii, S. A friction controllable sliding isolation system, *J. Eng. Mech., ASCE*, 1993, **119**(6), in press.
13. Feng, Q. & Shinozuka, M. Use of variable damper for hybrid control of bridge response under earthquakes, *Proc. US National Workshop on Structural Control Research*, Los Angeles, CA, 1991, pp. 107–12.
14. Kelly, J.M., Lopez, A.F., Inuadi, J. & Rodellar, J. Predictive control of base isolated structures, *Earth. Eng. Struct. Dyn.*, 1992, **21**(6), 471–82.
15. Nagarajaiah, S., Riley, M.A. & Reinhorn, A. Control of sliding isolated bridges with absolute acceleration feedback, *J. Eng. Mech., ASCE*, 1993, **119**(11), in press.
16. Reinhorn, A.M., Manolis, G.D. & Wen, C.Y. Active control of inelastic structures. *J. Eng. Mech., ASCE*, 1987, **113**(3), 315–33.
17. Yang, J.N., Li, Z., Danielians, A. Liu, S.C. Aseismic hybrid control of nonlinear and hysteretic structures I, *J. Eng. Mech., ASCE*, 1992, **118**(7), 1423–40.
18. Feng, Q., Shinozuka, M., Fujii, S. & Fujita, T. A hybrid isolation system for bridges, *Proc. 1st US–Japan Workshop on Earthquake Protection Systems for Bridges*, Buffalo, NY, 4–5 September 1991.
19. Nagarajaiah, S., Riley, M., Reinhorn, A. & Shinozuka, M. Hybrid control of sliding isolated bridges, *Proc. 1992 Pressure Vessels and Piping Conf., ASME*, 1992, PVP-237-2, pp. 83–9.
20. Subramaniam, R., Reinhorn, A.M. & Nagarajaiah, S. Application of fuzzy set theory to the active control of base isolated structures, *Proc. US/China/Japan Trilateral Workshop on Structural Control*, China, Shanghai, 3–7 October 1992, pp. 153–9.
21. Nagarajaiah, S., Feng, Q., Shinozuka, M. & Reinhorn, A. Analysis of bridges with friction-controllable sliding isolation system, *Proc. 3rd NSF Workshop on Bridge Engineering Research in Progress*, University of California, San Diego, 1992, pp. 243–6.
22. Masri, S.F., Bekey, G.A. & Caughey, T.K. On-line control of nonlinear flexible structures, *J. Appl. Mech., ASME*, 1981, **49**(4), 871–84.
23. Yang, J.N., Long, F.X. & Wong, D. Optimal control of nonlinear structures, *J. Appl. Mech.*, 1988, **55**(4), 931–8.
24. Wen, Y.K. Methods of random vibration for hysteretic structures, *J. Eng. Mech., ASCE*, 1989, **102**(2), 249–63.